2. Topocentric Angular Speed of Space Debris

In this chapter, the observational geometry for the full range of viewing angles from a telescope on the Earth's surface is examined, to determine the range of topocentric angular speed of space debris in different orbits that will be present in the sky. This knowledge is used to characterise the velocity regime likely to be encountered by any debris detection system pointing at any area in the sky. The line-of-sight vector is referred to as the "look angle" in this text.

The instantaneous topocentric angular speed of space debris ("ω_{top}") observed perpendicular to the observer's look angle is important to debris detection, as the more time that debris spends in the telescope's field of view, the greater its chances are of being detected.

Angular speed is referred to rather than angular velocity because it is mainly the magnitude of the angular velocity that is important to detection in terms of dwell time in the CCD pixel's field of view. In chapter 7 the direction as well as the magnitude of the angular velocity vector becomes important in terms of the debris' dwell time across the entire rectangular array of the CCD.

As most of the chapters in this thesis require some knowledge of the angular speed of space debris, this chapter investigates the range of ω_{top} expected from all configurations of observing site and debris orbit possible. It approaches the problem from a simple zenith-pointing two-dimensional case, and progresses to a more complex non-zenith-pointing three-dimensional case.

2.1 Topocentric and geocentric angular speed

The topocentric angular speed of a debris object is its apparent angular speed relative to the observer. It may be very different to the angular speed of the debris relative to the centre of the Earth, its 'geocentric' angular speed ω_d, but nevertheless is of primary concern to this investigation.

The means of deriving ω_{top} from ω_d is always the same no matter what the circumstances. The value of ω_{top} is obtained by calculating the linear velocity v_d of the debris then calculating the apparent angular velocity ω_{top} of that debris as seen by the observer, usually much closer to the debris than the Earth's centre. The linear velocity remains unchanged despite a change of viewpoint (Figure 2.1). With

reference to Figure 2.1 the linear velocity v is calculated by multiplying ω_g by the radius vector of the orbit, R:

$$v = \omega_d R . \quad (2.1)$$

The topocentric angular speed is then calculated by dividing the linear velocity v by the distance between the debris and the observer (s) ,

$$\omega_{top} = v/s = \omega_d R / s . \quad (2.2)$$

For the special case of the debris being at the observer's zenith, figure 3.1 is two-dimensional and $R = r_e + s$. If the orbit is also circular, the distance s is just the orbit height.

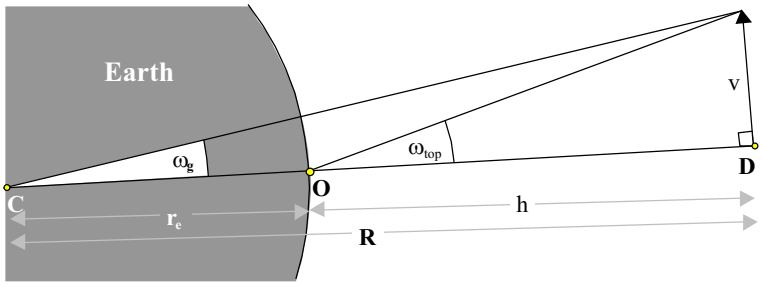

Figure 2.1: Basic premise behind geocentric and topocentric angular speed. Debris at D at orbital height h (radius R) moves at linear velocity v. The observer is at O and the centre of the Earth is marked at C. The geocentric angular speed ω_d is smaller than the topocentric angular speed ω_{top} due to the observer's closer proximity to the debris. Small angles for instantaneous velocity treatment are greatly exaggerated in this figure for clarity.

The fact that the Earth rotates complicates matters only slightly in that one must redefine the geocentric angular speed to be not just that provided by the debris' orbital angular velocity ω_g, but that of the vector addition result of ω_d and the sidereal rate apparent in the observer's field of view. This rate is governed by the declination of the point where the observer-debris line of sight vector (the "look angle") is projected to meet the celestial sphere – the "topocentric declination". The calculations for the general case are presented in detail in section 2.3.2, but for now the main point to consider is that this vector sum modification means that the ω_d factor in equation (2.2) is replaced by a resultant vector ω_r. However, the linear velocity and subsequent topocentric angular speed are calculated in the same manner; hence from (2.2):

$$\omega_{top} = \omega_r R / s . \quad (2.3)$$

In the simple coplanar scenarios outlined in the next two sections, the value of ω_r is obtained by simple subtraction.

2.2 Observing at the zenith

The simplest case to discuss involves the telescope pointing at the zenith. This not only simplifies the maths, but also serves a major purpose in that the optical path traverses the least amount of atmosphere in this direction, thus minimising atmospheric absorption and optimising conditions for viewing faint objects.

2.2.1 Definition of ω_{top} - general 2D case

Consider the 2-D case of a body P in circular Earth orbit above the equator, with an observer O also on the equator watching the body pass through its zenith (Figure 2.2). The orbit is prograde (as most satellite & therefore debris orbits are), i.e. anticlockwise as viewed from above the North Pole. The geocentric orbital velocity of P, (v_p) is given by:

$$v_p = \sqrt{\frac{\mu}{R}} \text{ m s}^{-1}, \tag{2.4}$$

where $\mu = GM_e$ (G = gravitational constant = 6.673×10^{-11} N m^2 kg^{-2}, M_e = Mass of Earth = 5.98×10^{24} kg), and R = orbit radius = r_e + h, where r_e = Earth equatorial radius = 6378 km, and h = orbit height (km).

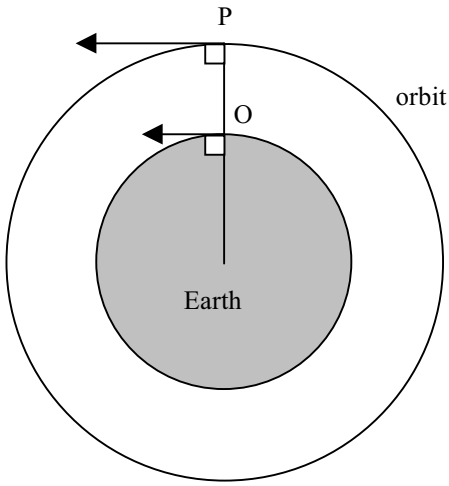

Figure 2.2 Two-dimensional case of topocentric angular speed (c.f. Figure 2.1).

Given the relationship between linear and angular speed $\omega = v/r$, where r = radius and v = linear velocity, the angular speed of the body P with respect to the Earth's centre, i.e. its geocentric angular speed ω_g, is given by:

$$\omega_d = \frac{v_p}{R} = \sqrt{\frac{\mu}{R^3}} \text{ radians s}^{-1}. \tag{2.5}$$

The Earth revolves about its axis in one sidereal day (86164.09s), so the geocentric

angular speed ω_o of the observer O at the equator is given by the Earth's sidereal rate ω_{sid}; i.e. $\omega_o = \omega_{sid}$ (in this case only), where:

$$\omega_{sid} = \frac{2\pi}{86164.09} = 7.292\times10^{-5} \text{ radians s}^{-1}. \quad (2.6)$$

Adopting a rotating frame of reference with the observer, the relative geocentric angular speed ω_r of point P relative to point O is therefore:

$$\omega_r = \omega_d - \omega_o = \sqrt{\frac{\mu}{R^3}} - \omega_o \text{ radians s}^{-1}. \quad (2.7)$$

The relative, or topocentric, linear velocity of P with respect to O during passage through the zenith, i.e. at the instant when the radius vectors of P and O align, is given by:

$$v_{rel} = R\,\omega_r = R\left[\sqrt{\frac{\mu}{R^3}} - \omega_o\right] \text{ m s}^{-1}. \quad (2.8)$$

The topocentric angular speed of P is therefore just:

$$\omega_{top} = \frac{v_{rel}}{h} = \frac{R}{h}\left[\sqrt{\frac{\mu}{R^3}} - \omega_o\right] \text{ radians s}^{-1}, \quad (2.9)$$

which in terms of the original orbital velocity is:

$$\omega_{top} = \frac{v_{rel}}{h} = \frac{R}{h}\left[\frac{v_p}{R} - \omega_o\right] \text{ radians s}^{-1}. \quad (2.10)$$

Note that ω_{top} goes to zero for:

$$R = \left(\frac{\mu}{\omega_o^{\,2}}\right)^{\frac{1}{3}} \text{m}, \quad (2.11)$$

which is the orbital radius for geostationary communications satellites. For the values given above, the radius is 42,173km, or a height of 35,795km (Figure 2.3).

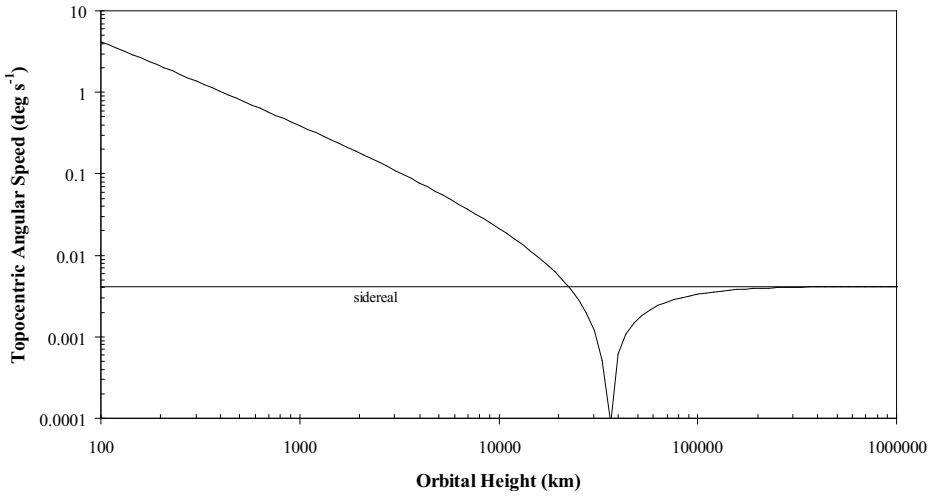

Figure 2.3 Topocentric angular speed at zenith for 2D equatorial case only, with circular orbit. Note the asymptote at sidereal rate; for extremely high orbits above GSO the geocentric angular speed is very small so that the effect due to the Earth's rotation dominates. However, the Earth's sphere of influence only extends to ~10^6 km, so in practice orbits above this height would be unstable (Roy, 1988), (Weisel, 1989). The dip at geostationary orbit (GSO) is explained in the text.

2.2.2 Extremes of topocentric angular speed

In order to characterise the full range of ω_{top}, the slowest and fastest possible topocentric angular velocities must be determined. Apart from the special case of GSO, the slowest case of ω_{top} can be characterised as the apogee of an elliptical prograde orbit, while the fastest can be thought of as the perigee of a retrograde parabolic orbit. By definition, an object in a parabolic orbit is moving at escape velocity, and although it is not worthwhile looking for debris in such orbits, it does represent the upper limit of angular speed. The elliptical orbit case has its perigee fixed at a suitably low altitude, because for a given apogee, the lower the perigee, the slower the speed at apogee. The lowest perigee height permissible for a relatively stable orbit would be that of a typical LEO, so a perigee height of 200km was chosen for this exercise.

The calculation of ω_{top} for these cases is very similar to that for the circular orbit case, the differences arising from different expressions for the orbital velocity at height h. For the elliptical orbit, the apogee velocity is given by:

$$v_{apo} = \sqrt{\frac{\mu}{a}\left(\frac{1-e}{1+e}\right)} \text{ m s}^{-1}, \tag{2.12}$$

where a = semimajor axis of orbit, e = eccentricity of orbit. If the height of perigee and apogee are given by h_p and h_a respectively, then with reference to Figure 2.4,

terms involving a and e can be rewritten using:

$$a = \frac{2r_e + h_p + h_a}{2}, \tag{2.13}$$

$$a(1-e) = r_e + h_p \quad \Rightarrow \quad (1-e) = \frac{r_e + h_p}{a}, \tag{2.14}$$

$$a(1+e) = r_e + h_a \quad \Rightarrow \quad (1+e) = \frac{r_e + h_a}{a}, \tag{2.15}$$

so that equation (2.12) can be rewritten as:

$$v_{apo} = \left\{ \frac{2\mu}{\left(2r_e + h_p + h_a\right)} \left[\frac{r_e + h_p}{r_e + h_a} \right] \right\}^{\frac{1}{2}} \text{ m s}^{-1}. \tag{2.16}$$

The parabolic case is simpler; by definition, escape velocity at any height above the Earth is simply √2 times what it would be in a circular orbit, treating that position as the perigee. Thus the parabolic velocity at height h is:

$$v_{para} = \sqrt{\frac{2\mu}{R}} = \sqrt{\frac{2\mu}{\left(r_e + h\right)}} \text{ m s}^{-1}. \tag{2.17}$$

Incorporating equations (2.16) and (2.17) into (2.10), we obtain the topocentric angular speed expressions for the two extreme cases:

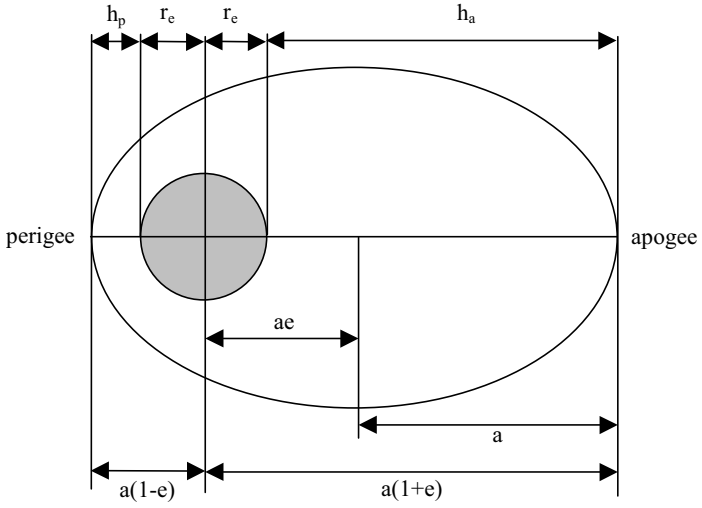

Figure 2.4 Orbit parameters in terms of apogee/perigee heights. See text for details.

$$\omega_{top_{apo}} = \frac{R}{h} \left\{ \left[\frac{2\mu R_{peri}}{R^3 \left(R_{peri} + R\right)} \right]^{\frac{1}{2}} - \omega_o \right\} \text{ radians s}^{-1}, \tag{2.18}$$

$$\omega_{top_{para}} = \frac{R}{h}\left\{\left[\frac{2\mu}{R^3}\right]^{\frac{1}{2}} - \omega_o\right\} \text{ radians s}^{-1}, \qquad (2.19)$$

where $R = r_e + h_a$ and $R_{peri} = r_e + h_p$ for the elliptical case. Plotting these with respect to height gives Figure 2.5.

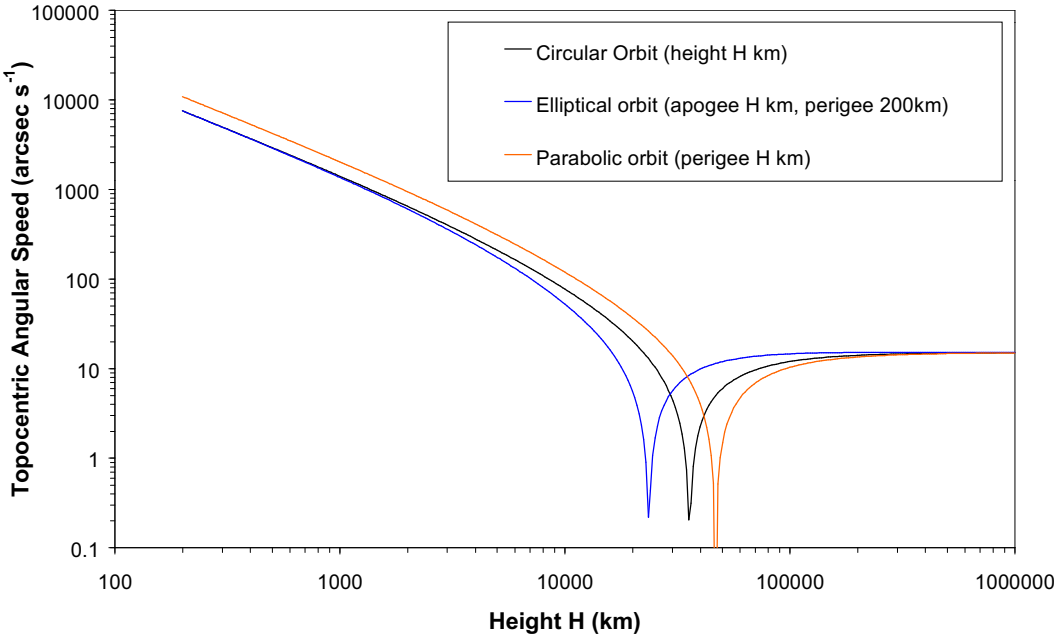

Figure 2.5 Extremes of topocentric angular speed, represented by elliptical orbit apogee (slowest) to parabolic perigee (fastest) - see text. Nonzero minima caused by sampling frequency.

2.2.3 Three-dimensional case: i≠0, zenith-looking observatory at latitude L≠0, and circular orbit.

The basic tenet behind the calculation remains the same but with some subtle differences. With reference to Figure 2.6, the celestial sphere is represented, showing the debris orbit as a great circle inclined at angle i to the equator, with the path of the observer made as the Earth revolves at latitude L as a small circle. More precisely, the observer's path is that of its zenith projected on the celestial sphere. The point of intersection is marked at X.

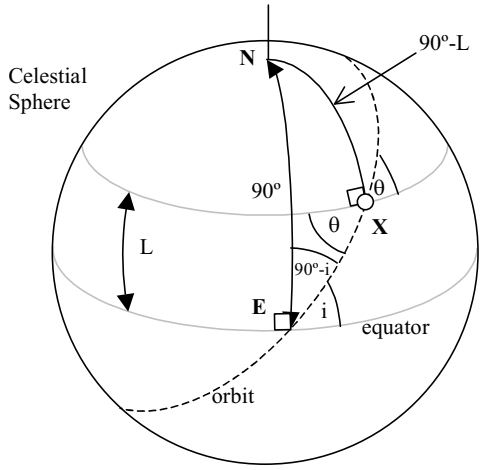

Figure 2.6: Three-dimensional treatment of topocentric angular velocity at zenith for non-zero latitude and inclination. See text for details.

The angle θ between the geocentric angular speed vector of the debris and the observer's zenith can be found by solving the spherical triangle NEX using the spherical sine rule:

$$\frac{\sin(90° - L)}{\sin(90° - i)} = \frac{\sin 90°}{\sin(90° + \theta)}, \tag{2.20}$$

$$\therefore \frac{\cos L}{\cos i} = \frac{1}{\cos \theta}, \tag{2.21}$$

$$\therefore \theta = \cos^{-1}\left[\frac{\cos i}{\cos L}\right]. \tag{2.22}$$

The relative geocentric angular speed of the debris at the observer's zenith is therefore found by vector addition of the geocentric angular velocities of the debris (ω_d) and of the observer's zenith point (ω_z), where:

$$\omega_z = \omega_{sid} \cos L, \tag{2.23}$$

and ω_z is a special case of the topocentric declination of the debris (the more general case is defined in section 2.3.2).

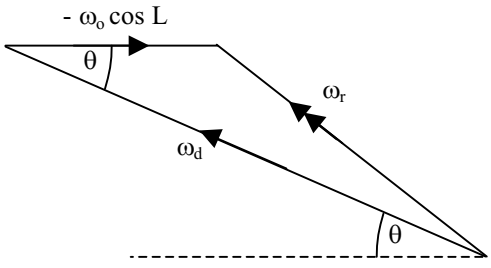

Figure 2.7 Vector addition of instantaneous geocentric velocity of debris and observer.

With reference to Figure 2.7, the magnitude of the resultant is given by the two-

dimensional cosine rule, since velocities are instantaneous in this situation and therefore the spherical triangle in Figure 2.7 is infinitesimally small and can be approximated by a two-dimensional triangle. The resultant magnitude is therefore:

$$\omega_r = \left[\omega_d{}^2 + (\omega_o \cos L)^2 - 2\omega_d\omega_o \cos L \cos\theta\right]^{\frac{1}{2}} \text{ radians s}^{-1}. \qquad (2.24)$$

As before in the 2D case, this resultant geocentric angular speed has a corresponding geocentric linear velocity $v_r = R\ \omega_r$, and relative to the observer distance h from the debris (as we are considering the debris at the zenith), the topocentric angular speed is therefore:

$$\omega_{top} = \frac{v_r}{h} = \frac{R}{h}\left[\omega_d{}^2 + (\omega_o \cos L)^2 - 2\omega_d\omega_o \cos L \cos\theta\right]^{\frac{1}{2}} \text{ radians s}^{-1}. \qquad (2.25)$$

But from equation (2.22), $\cos\theta = \cos i / \cos L$, therefore (2.25) becomes:

$$\omega_{top} = \frac{R}{h}\left[\omega_d{}^2 + (\omega_o \cos L)^2 - 2\omega_d\omega_o \cos i\right]^{\frac{1}{2}} \text{ radians s}^{-1}. \qquad (2.26)$$

As a check, putting L = i = 0 should result in the 2D equatorial equation given in (2.10). Substituting in the values of L and i into (2.26) gives:

$$\begin{aligned} \omega_{top} &= \frac{R}{h}\left[\omega_d{}^2 + \omega_o{}^2 - 2\omega_d\omega_o\right]^{\frac{1}{2}} \\ &= \frac{R}{h}\left[(\omega_d - \omega_o)^2\right]^{\frac{1}{2}} \\ &= \frac{R}{h}\left[\omega_d - \omega_o\right] \end{aligned} \qquad (2.27)$$

as before (as $\omega_d = v_p/R$).

We are now in a position to investigate the effects orbit inclination and observer latitude has on topocentric angular speed at the observer's zenith. Figure 2.8 shows the variation of ω_{top} with latitude and inclination for a circular LEO of 200km. The wedge shape is due to the orbit not being visible at the zenith for latitudes greater than the inclination of the orbit. The value calculated earlier for the simple 2D coplanar case is seen reproduced at the bottom of the surface, at inclination = 0º, latitude = 0º.

For a constant latitude ω_{top} increases with orbital inclination as the orbit vector moves round to oppose the zenith vector. For a constant inclination, the effect of changing latitude is slight for LEO orbits as $\omega_d \gg \omega_o$, but for higher orbits the effect is more evident, as witnessed in Figure 2.9 and Figure 2.10. The effect of stationary

ω_{top} at GSO is also seen from the dip at i = 0º in Figure 2.10.

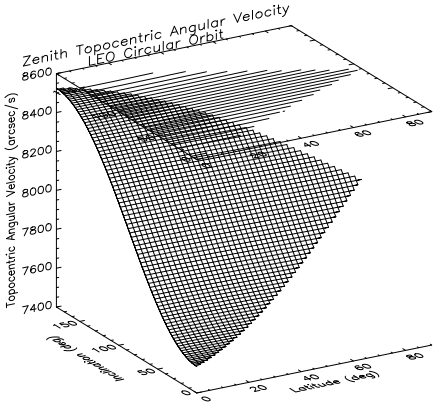

Figure 2.8: ω_{top} for LEO

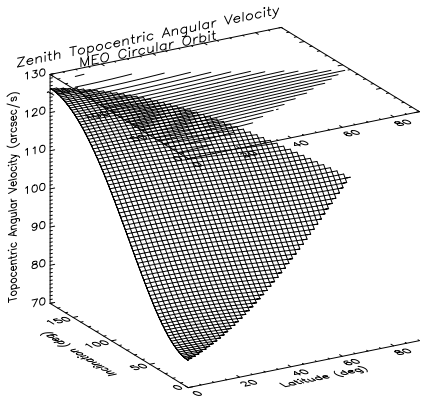

Figure 2.9: ω_{top} for higher orbit (10,000km)

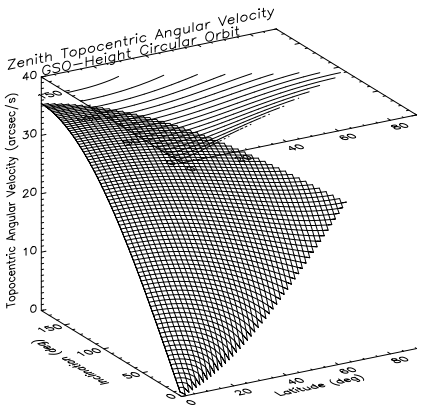

Figure 2.10: ω_{top} for GSO

2.3 Away from the zenith

2.3.1 Trajectory through zenith (2D)

At non-zero zenith angles the linear velocity of the debris is foreshortened along the observer's line of sight (Figure 2.11); this has the effect of reducing ω_{top} below its value at the zenith. The main disadvantage however is that by staring through a thicker amount of atmosphere the brightness of the object is reduced by atmospheric extinction, which compromises detection. That aspect of debris detection is addressed in chapter 4 however; the remainder of this chapter concentrates on angular speed only. Starting with the simple case of a 2D coplanar

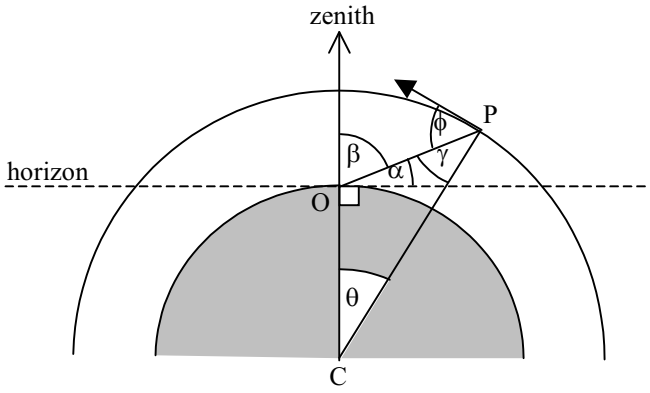

Figure 2.11 : Foreshortening effect on topocentric angular speed for non-zenith considerations.

equatorial case again, (Figure 2.11), ω_{top} at a zenith angle β for a circular orbit is calculated by defining the angle the velocity vector makes with the observer's line-of-sight (line OP in the figure). The linear velocity of the debris relative to the observer is as before (following equation (2.1)):

$$v_{rel} = (r_e + h) - (\omega_g - \omega_o) \, . \tag{2.28}$$

The velocity component perpendicular to the line of sight ($v_\perp$) is what determines the apparent topocentric angular speed, and is given simply by:

$$v_\perp = v_{rel} \sin \phi = (r_e + h) - (\omega_g - \omega_o) \ \sin \phi. \tag{2.29}$$

Hence the topocentric angular speed is given by $v_\perp$ divided by the distance between the object and observer, in this case the slant range denoted by OP in Figure 2.11:

$$\omega_{top} = \frac{v_\perp}{OP} = \frac{(r_e + h)(\omega_g - \omega_o) \sin \phi}{OP}. \tag{2.30}$$

Using the sine rule to solve triangle POC, we obtain:

$$\sin \gamma = \frac{r_e}{R} \cdot \sin(90 + \alpha) \tag{2.31}$$

$$\therefore \cos \phi = \frac{r_e}{R} \cdot \cos \alpha \tag{2.32}$$

$$\therefore \sin \phi = \left[1 - \left(\frac{r_e}{R} \cdot \cos \alpha \right)^2 \right]^{\frac{1}{2}}. \tag{2.33}$$

The distance OP is found from the cosine rule:

$$OP^2 = r_e^2 + R^2 - 2 \, r_e \, R \cos \theta, \tag{2.34}$$

so

$$OP^2 = r_e^2 + R^2 - 2 \, r_e \, R \cos (\pi - \alpha - \phi) \, . \tag{2.35}$$

The resulting behaviour of ω_{top} with zenith angle for a pass through the zenith is

shown in Figure 2.12. It can be seen that for LEO orbits ω_{top} falls by over an order of magnitude compared to its value at the zenith.

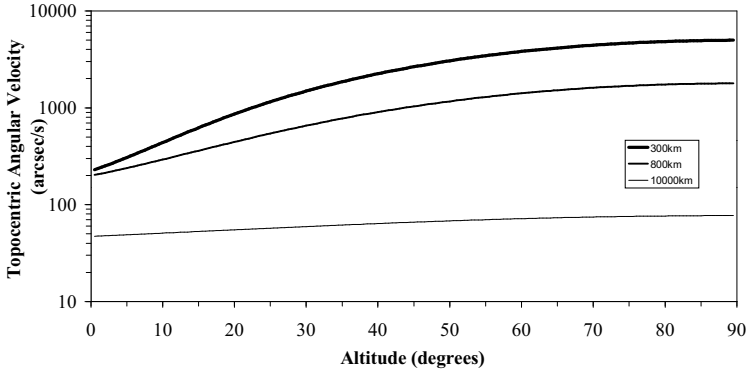

Figure 2.12 Topocentric angular speed as a function of altitude (angular distance above horizon) for circular orbit and various heights. Note the fall by about an order of magnitude near the horizon for LEO.

This can be seen more clearly by calculating the ratio of ω_{top} away from the zenith, over ω_{top} at the zenith. In Figure 2.13 it can be seen that for circular orbits (again in the 2D case), the greatest reduction in ω_{top} occurs for large zenith distances and low orbits.

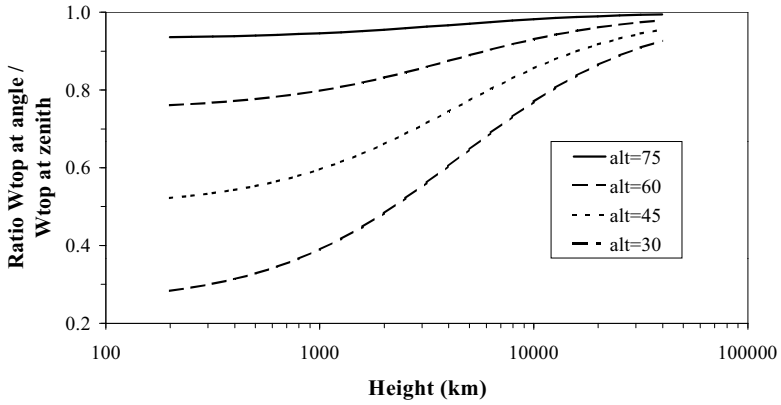

Figure 2.13 Ratio of angular speed at a given zenith angle to that at zenith.

2.3.2 Non-Zenith Pass (3D)

The final scenario considered in this chapter concerns itself with the most general case of a debris pass, that where the debris does not pass through the observer's zenith. For the sake of simplicity the orbit remains circular and we will consider only the moment of closest approach, and hence of maximum topocentric angular speed.

Consider the situation outlined in Figure 2.14 of an "orbit sphere" concentric with the Earth's surface, with a radius equal to that of the debris orbit. The height of

this sphere above the Earth's surface is therefore equal to the orbit height. An observer at O has their zenith point defined as being the observer's radius vector extended to meet the orbit sphere at ZP. A zenith angle z therefore has a corresponding geocentric zenith angle θ of:

$$\theta = z - \sin^{-1}\left[\frac{r_e}{R}\sin(\pi - z)\right], \tag{2.36}$$

with $R = r_e + h$. The loci of zenith angles about the observer at O is therefore denoted by the dashed small circle with radius θ in Figure 2.14. With reference to Figure 2.15, which shows only the orbit sphere for clarity, for the orbit path to satisfy the condition of passing by the observer at the zenith angle specified, it must only meet the zenith circle tangentially at point Z and not cross it.

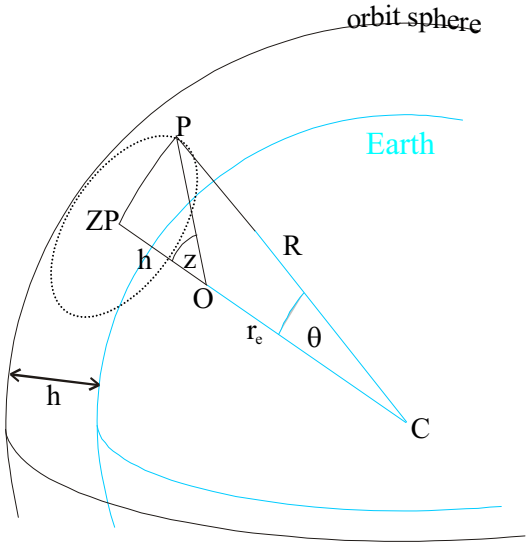

Figure 2.14 Geometry for orbit sphere calculations. See text for details.

To calculate the relative angular speed the sidereal component is found first; this is obtained by calculating the declination of the point Z, since as before the magnitude of sidereal motion due to the Earth's rotation depends on the declination by $\omega_o = \omega_{sid} \cos \delta$. The declination in question however is the topocentric declination, which in the case of an Earth satellite may be many degrees (up to 90º) different from the declination as viewed from the Earth's centre (geocentric declination). This is a topocentric parallax effect caused by the finite radius of the Earth. For astronomical work, where the distance to the observed object is >> r_e, the parallax effect is slight, amounting to just a few seconds of arc for the planets, and almost 1º for the Moon.

The calculation to find the topocentric declination proceeds first with finding the

geocentric declination. In Figure 2.15, the orbit plane is tilted with respect to the celestial equator by its inclination i. The pole of the orbit is therefore denoted by K, and the angle between the celestial pole and that of the orbit plane is i. The problem then begins to resemble a coordinate transformation between celestial coordinates and those based in the orbit plane.

The great circle arc XZ by definition is perpendicular to the orbit plane, being the radius of the small circle to which the orbit plane is tangent. Extending XZ up to meet the orbit pole at K makes XK 90º. The latitude of the observer is given by angle AZ, and the declination of the closest approach is shown as BX. Extending both of these arcs to cross XK and meet the celestial pole at P creates two spherical triangles, ΔKPX and ΔKPZ.

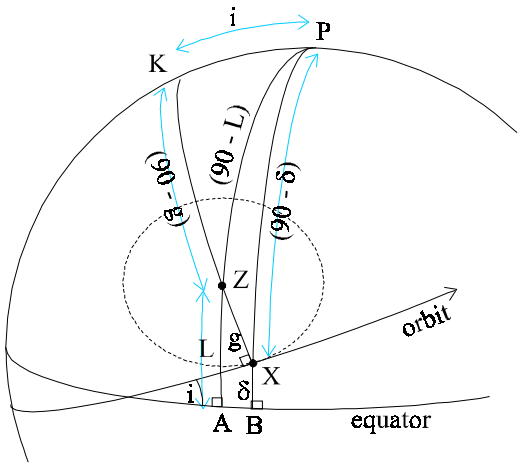

Figure 2.15 Geometry for non-zenith closest approach, showing small circle of zenith angle loci for observer (dotted circle).

It can be seen that ∠ZKP is common to both triangles, and can be found using the spherical cosine formula for ΔKPZ, all sides of which are known. Therefore,

$$\cos \angle ZKP = \left[\frac{(\sin L - \sin g \cos i)}{\cos g \sin i} \right]. \tag{2.37}$$

Given ∠ZKP, ΔKPX can now be solved using the spherical cosine formula again:

$$\cos(90 - \delta) = \cos 90 \cos i + \sin 90 \sin i \cos \angle ZKP \tag{2.38}$$

$$\therefore \sin \delta = \sin i \cos \angle ZKP \tag{2.39}$$

$$\therefore \sin \delta = \frac{\sin i (\sin L - \sin g \cos i)}{\cos g \sin i} \tag{2.40}$$

To correct for topocentric parallax, the following construction is used (Figure 2.16). In this case only the vectors pointing to the observer and the debris are shown (this is not a spherical trigonometry problem). The reference system AYP is

aligned with the celestial sphere, i.e. the celestial equator lies in the AY plane (with A pointing to the vernal equinox, though strictly speaking this is not necessary), and P pointing to the north celestial pole.

The debris is at point Q, the observer at point O and the centre of the Earth at point C. The geocentric declination found in equation (2.40) and depicted in Figure 2.15 is shown as δ_g while the topocentric declination is δ_t. The local non-rotating coordinate system at O has axes parallel to the central axes. Perpendiculars from Q and O (QB & OD respectively) are dropped to the celestial equatorial plane and by definition the angles ∠CBQ and ∠CDO are both 90º.

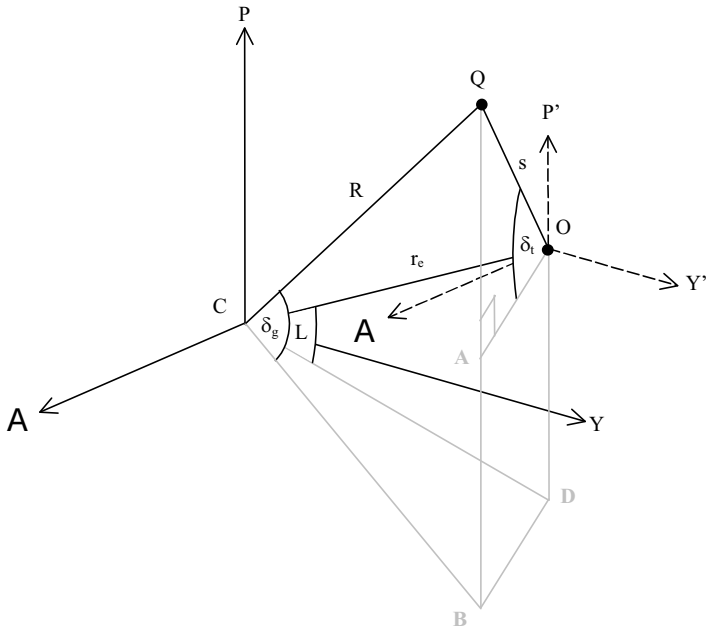

Figure 2.16 Topocentric parallax correction

The triangles ΔCBQ and ΔCDO are both solvable however, since the hypotenuse of both are R and r_e respectively. Therefore the height above the celestial equatorial plane of the observer (DO) is given simply by DO = r_e sin L, and that of the debris is BQ = R sin δ_g . Since QB and OD are parallel, the distance above the local celestial equatorial plane at O is simply QA = (QB - OD). This makes the triangle ΔAOQ solvable since the hypotenuse OQ is also known, being the observer-debris distance (s). Therefore the topocentric declination δ_t is given by:

$$\delta_t = \sin^{-1}\left[\frac{QA}{s}\right] \tag{2.41}$$

$$= \sin^{-1}\left[\frac{R \sin \delta_g - r_e \sin L}{s}\right] \tag{2.42}$$

Given this declination, the magnitude of sidereal motion at that look angle is therefore $\omega_o = \omega_{sid} \cos \delta_t$. The relative angular speed is found as before by the cosine rule in Figure 2.7. The angular speed of debris at a non-zenith closest approach is shown in Figure 2.17, Figure 2.18 and Figure 2.19 for a range of debris heights and zenith distances.

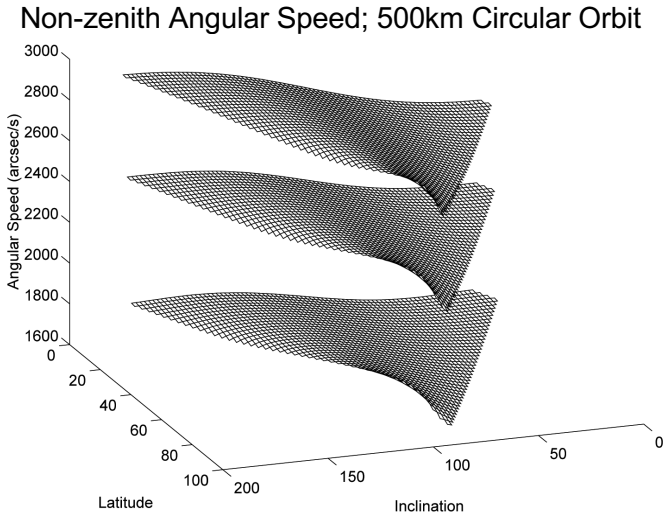

Figure 2.17: Topocentric angular speed for zenith angles of 30º (upper surface), 45º (middle surface), and 60º (lower surface), for the latitude range 0º-90º N, and inclination range 0º-180º. Note the reversed inclination axis.

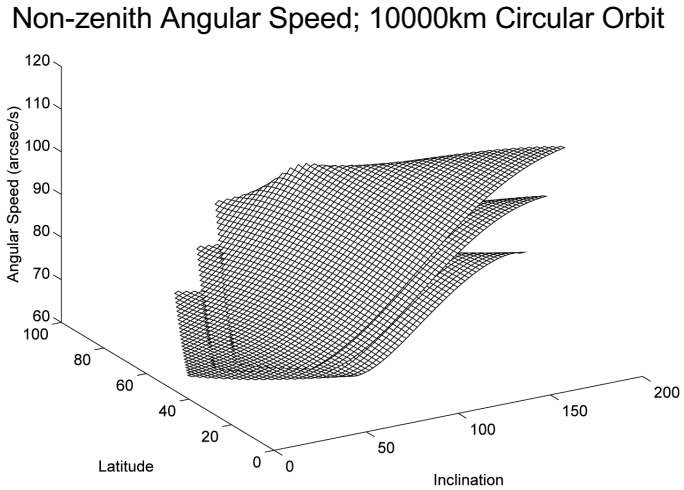

Figure 2.18: Same as for Figure 2.17 but for orbital height of 10,000km.

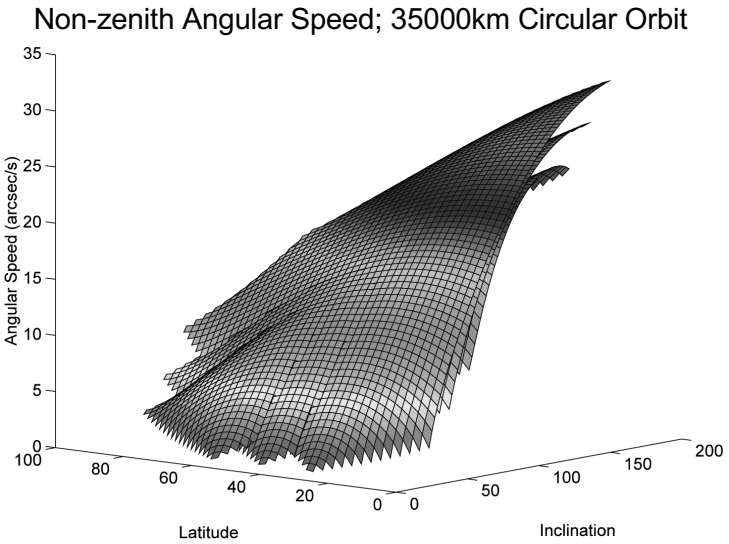

Figure 2.19: Same as for Figure 2.17, but for a near GSO orbital height of 35,000km.

It can be seen in Figure 2.17 that the effect of changing orbit inclination is to increase ω_{top} for retrograde orbits. The effect of inclination is small compared to the absolute value of ω_{top}. This is because the geocentric angular speed ω_d in LEO is much greater than ω_o, so the inclination-induced angular difference at the zenith has little effect. The pattern is repeated further from the zenith, but for lower absolute values due to foreshortening.

The overall pattern is similar in Figure 2.18; but the relative effect of increasing inclination is greater for these curves, because ω_d is smaller while ω_o remains the same. For near-GSO orbits however, where $\omega_d \sim \omega_o$, the effects of inclination are the most pronounced and produce intersecting curves as shown in Figure 2.19.

2.4 Conclusions

Topocentric angular speed "ω_{top}" was defined and calculated for a variety of orbital inclinations, observing latitudes and viewing angles, for the purpose of getting a feel for the range of angular speeds likely to be encountered by a ground-based debris detection system.

It was found that for a given latitude of observing site, ω_{top} always increased with orbital inclination and decreased with increasing zenith distance due to geometry, and decreased with orbital height due to the slower orbital speeds.